Non-cardinal color mechanism elicitation by stimulus shape: Bringing the S versus L+M color plane to the table

Karen L. Gunther

Psychology Department, Wabash College, Crawfordsville, IN, USA

Neurons in the cortex typically respond best to elongated stimuli, or gratings, whereas neurons in the lateral geniculate nucleus (LGN) typically prefer circular stimuli, or spots. Further, neural mechanisms specifically tuned for non-cardinal colors largely do not emerge until the cortex; therefore, the use of gratings should better reveal non-cardinal color mechanisms. This hypothesis has been tested in the isoluminant color plane in macaque monkeys (Stoughton, Lafer-Sousa, Gagin, & Conway, 2012) and in the L–M versus L+M color plane in human subjects (Gegenfurtner & Kiper, 1992). Here, this hypothesis was tested in the third color plane, S versus L+M, in human subjects in two experiments. Experiment 1 tested 10 subjects across four directions in this color plane; Experiment 2 tested three subjects in eight to twelve color directions. Consistent with data from the other two color planes, in both experiments in the S versus L+M color plane, gratings revealed the presence of non-cardinal mechanisms more strongly than did spots.

Introduction

In nature, how do our brains perceive a round bluish delphinium blossom or the horizon between a bright blue sky and the amber waves of grain? The bluish-purple of the delphinium blossom is considered to be a "cardinal" color, whereas bright sky blue and deep amber yellow are considered to be "non-cardinal" colors. Cardinal colors are reddish, greenish, bluish, yellowish, black, and white. These colors can be represented by their cone inputs: reddish as L–M, greenish as –L+M, bluish as S+, yellowish as S–, black as –L–M, and white as L+M, with L representing the long-wavelength-sensitive cones, M representing the medium-wavelength-sensitive cones, and S representing the short-wavelength-sensitive cones. These six colors are designated as "cardinal" because there are cell types early in visual processing, in the retina and lateral geniculate nucleus of the thalamus, that respond best to these colors: L–M and –L+M are primarily underlain by the midget retinal ganglion cells (RGCs) and parvo lateral geniculate nucleus (LGN) of the thalamus cells; S+ and S– are primarily underlain by the small bistratified RGCs and konio LGN cells; and –L–M and L+M are underlain by the parasol RGCs and magno LGN cells or, in some cases, the midget/parvo pathway. All color directions beyond these three axes (including the bright blue sky and deep amber grains) are known as non-cardinal, and their neural mechanisms largely do not emerge until the cortex (DeValois, Cottaris, Elfar, Mahon, & Wilson, 2000; Gegenfurtner, 2003). (Note that the S+/S– pathway may be comprised of distinct S+ and S– pathways, and that S– LGN neurons have been shown to respond to a wide range of colors around 90° in Derrington, Krauskopf, and Lennie (DKL) space (e.g., Tailby, Solomon, & Lennie, 2008; Wool, Packer, Zaidi, & Dacey, 2019). Thus, S– LGN neurons may be responding to non-cardinal colors.)

The ability to reveal the presence of mechanisms tuned to respond to non-cardinal colors has varied across studies (for reviews, see Eskew, 2009; Gunther, 2014a). Not only do neurons at the different levels of processing (retina and LGN, versus cortex) show differential color tuning, but they also prefer stimuli of different shapes. Retinal and geniculate neurons respond best to circular spots (like the delphinium blossom), whereas cortical neurons respond better to gratings, lines, or bars (like the horizon between the blue sky and the amber grains) (Conway, Chatterjee, Field, Horwitz, Johnson, Koida, & Mancuso, 2010). Although the signals for all types of visual stimuli must pass through the LGN on the way to the cortex and through the cortex to create a conscious percept, this use of differently shaped stimuli is often phrased as which stimulus is "more effective" at stimulating which neurons (e.g., Gegenfurtner & Kiper, 1992; Stoughton, Lafer-Sousa, Gagin, & Conway, 2012), thus concluding that the stimuli are neurally processed at that level of the visual system. The current study examines the effect that stimulus shape may have on eliciting non-cardinal mechanisms.

The current two experiments explore the use of homogeneous spots versus bipolar gratings in their ability to reveal non-cardinal colors. Given that neurons in the LGN respond better to spots but cortical neurons

Citation: Gunther, K. L. (2022). Non-cardinal color mechanism elicitation by stimulus shape: Bringing the S versus L+M color plane to the table. *Journal of Vision*, *22*(5):5, 1–15, https://doi.org/10.1167/jov.22.5.5.

https://doi.org/10.1167/jov.22.5.5 Received August 8, 2021; published April 13, 2022 ISSN 1534-7362

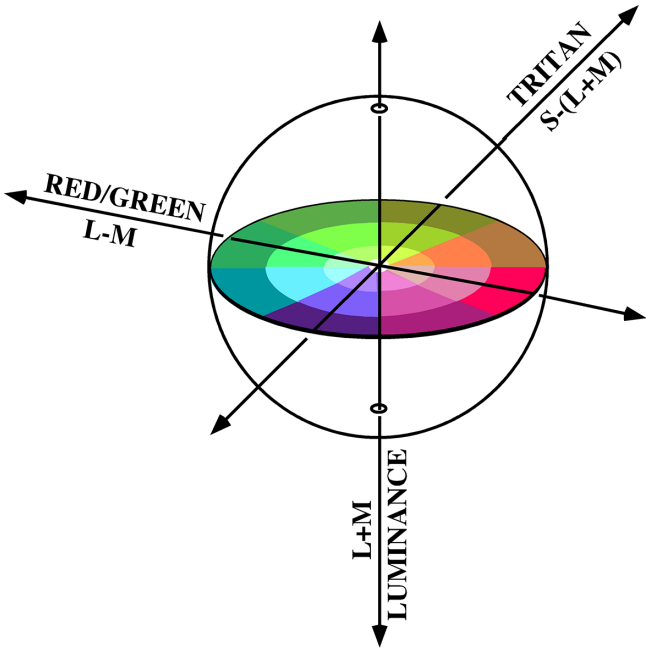

Figure 1. DKL three-dimensional color space. Red/green is underlain by L–M cone inputs, tritan is underlain by S, and luminance is underlain by L+M. Figure was modified from Gunther and Dobkins (2003).

respond better to gratings (Conway et al., 2010), and that non-cardinal mechanisms mostly do not emerge until the cortex (DeValois et al., 2000; Gegenfurtner, 2003) (but cf. Tailby et al., 2008; Wool et al., 2019), non-cardinal mechanisms should be more likely to be revealed with cortically stimulating gratings than with LGN-stimulating spots.

Two studies have in fact found stronger evidence for non-cardinal mechanisms when using gratings than when using spots, in two of the three planes of color space. A color space is a means to discuss color in a coherent manner. One three-dimensional representation of color space, shown in Figure 1, uses the cardinal opponent mechanisms (i.e., RGC or LGN cell preferences) as the cardinal axes: reddish/greenish is underlain by L–M, bluish/yellowish (i.e., tritan) is underlain by S, and luminance is underlain by L+M. This space is referred to as DKL space, after the pioneering work of Derrington, Krauskopf, and Lennie (1984). This color space can then be sliced into three cardinal planes: L–M versus S, or isoluminant (colored in Figure 1); L–M versus L+M; and S versus L+M. In the isoluminant plane, in macaque subjects, Stoughton and colleagues (2012) found evidence for non-cardinal mechanisms when adapting with grating stimuli but only slight evidence for non-cardinal mechanisms when adapting with full-field stimuli. Gegenfurtner and Kiper (1992) found non-cardinal mechanisms in the L–M versus L+M color plane when measuring detection thresholds for gratings but not when using 2°-diameter spots. To the best of the author's knowledge, the ability of spots versus gratings to reveal non-cardinal mechanisms has not yet been examined in the S versus L+M color plane (e.g., see relevant reviews by Eskew, 2009; Smithson, 2014). The S versus L+M color plane is examined in the current study.

Two studies with contradictory findings are those by Giulianini and Eskew (1998) and Sankeralli and Mullen (1997). In the L–M versus L+M plane, both studies found evidence only for cardinal mechanisms, whether using spots or gratings (Giulianini & Eskew, 1998) or gratings only (Sankeralli & Mullen, 1997). However, both sets of authors calculated their colors in cone contrast color space rather than DKL space (Figure 1). Cone contrast space calculates colors in terms of how much each cone type is stimulated by the stimulus versus by the background color. DKL color space calculates colors in terms of how much each post-receptoral mechanism (L–M, S, or L+M) is stimulated. This difference in representation of color space can alter the apparent distinctiveness of post-receptoral mechanisms. Hansen and Gegenfurtner (2013) point out that the stimuli used by Giulianini and Eskew, although the mechanisms appear to be quite distinct in cone contrast space, are very similar when mapped in DKL space, and all essentially only stimulate L–M. Further, when Sankeralli and Mullen replotted the data from Gegenfurtner and Kiper (1992) in cone contrast space, the evidence for non-cardinal mechanisms disappeared. Thus, the interpretation of whether non-cardinal mechanisms are present can be affected by the chosen color space, aside from the stimulus type (e.g., spots versus gratings) that is used.

The current study tests the hypothesis that gratings (that cortical neurons respond particularly well to) reveal non-cardinal colors better than do spots (that particularly stimulate LGN neurons), extending the examination of this hypothesis to the S versus L+M color plane. Experiment 1 tested this hypothesis in a larger number of subjects (10), but with fewer color axes (two cardinal and two non-cardinal per color plane). Experiment 2 tested this hypothesis in fewer subjects (three), but with eight ($n = 2$ subjects) or 12 ($n = 1$ subject) color axes per color plane.

Methods

The existence of separate mechanisms underlying different non-cardinal color axes was determined using noise masking, a common technique for studying non-cardinal mechanisms (Eskew, Newton, & Giulianini, 2001; Gegenfurtner & Kiper, 1992; Gunther, 2014a; Gunther & Downey, 2016; Hansen & Gegenfurtner, 2006; Hansen & Gegenfurtner, 2013; Li

& Lennie, 1997). In this technique, the spot or grating stimuli are presented in a field of pixelated noise. Noise masking reveals separate non-cardinal mechanisms if the contrast threshold to detect a stimulus when embedded in aligned noise is higher than when that same stimulus is embedded in orthogonal noise. Aligned noise is noise from the same color axis as the stimulus (e.g., 45° S versus L+M non-cardinal stimulus and noise, which appears as intense-bluish/dim-yellowish). Orthogonal noise is noise from the opposite color axis as the stimulus (e.g., 135° S versus L+M non-cardinal noise with the 45° S versus L+M non-cardinal stimulus; 135° appears intense-yellowish/dim-bluish).

The logic underlying the use of noise masking to study non-cardinal mechanisms is as follows. If separate neural mechanisms exist for the 45° and 135° non-cardinal stimuli, then the 45° mechanism would fire preferentially in response to the 45° stimulus, whereas the 135° mechanism would fire preferentially in response to the 135° noise. As far as the 45° mechanism is concerned, no noise is present (or very little, if the mechanisms and stimuli are not perfectly orthogonal), and the contrast required to detect the 45° stimulus would be low. On the other hand, if there are not specific mechanisms to detect the 45° and 135° non-cardinal mechanisms, then we are using the underlying cardinal mechanisms (e.g., S and L+M) to detect both the 45° and the 135° stimuli. In the case of detection by the cardinal mechanisms, the 45° non-cardinal stimulus and the 135° non-cardinal noise would both stimulate the S and L+M cardinal mechanisms, and the contrast of the 45° non-cardinal stimulus would have to be increased in order for its neural response to be "louder" than the neural response to the 135° non-cardinal noise, allowing the stimulus to be detected. Thus, the existence of independent non-cardinal mechanisms is determined by whether the detection of the 45° non-cardinal stimulus is affected more by the 45° non-cardinal noise than by the 135° non-cardinal noise. (Even if the orthogonal noise is not perfectly orthogonal to the neural mechanism that is detecting the stimulus, separate non-cardinal mechanisms are revealed when orthogonal, or nearly orthogonal, noise raises the stimulus threshold by less than does the aligned noise.)

Subjects

In Experiment 1, 10 subjects were tested, one female subject (48 years old) and nine male subjects (mean age 20.11 ± 1.45 years). Note that Wabash College has an all-male student body. Thus, the only female subject is the author. In Experiment 2, subject KLG (51 years old) participated again, plus two new male subjects (18 and 21 years old). For both experiments, normal color vision was verified by the Farnsworth-Munsell 100-Hue test (FM100). Error scores up to 100 are considered to reflect normal color vision; a stricter maximum error score of 50 was used in these studies. One subject in the S versus L+M color plane in Experiment 1 exceeded this threshold, with an overall error score of 88. However, his error score on the blue/yellow FM100 caps (Smith, Pokorny, & Pass, 1985) was 11, but his error score on the red/green caps was 77. This study was approved by the Wabash College Institutional Review Board, and all subjects gave written informed consent. The protocol conforms to the tenets of the Declaration of Helsinki.

Apparatus

In Experiment 1, stimuli were programmed in MATLAB (The MathWorks, Natick, MA), interfaced with the ViSaGe visual stimulus generator (Cambridge Research Systems, Rochester, UK) and presented on a 20-inch NEC MultiSync FP2141SB monitor (100-Hz refresh rate, 1024 × 768-pixel resolution; NEC Corporation, Tokyo, Japan). The calibration of the monitor was verified with a PR-655 Spectroradiometer (PhotoResearch, Syracuse, NY) or a ColorCAL (Cambridge Research Systems) each day on which a subject was tested, following a warm-up of at least 20 minutes with full screen gray at 24 cd/m^2. Any day on which the luminance values of the S+ and S– phases of the stimulus (at full contrast) were off by more than ±2% Michelson contrast—($LUM_{S+} - LUM_{S-}$)/($LUM_{S+} + LUM_{S-}$)—the monitor was recalibrated by linearizing the voltage/luminance relationship independently for each of the three phosphors (red, green, and blue), using the Gamma Correction System and a ColorCAL (both, Cambridge Research Systems). The Cambridge Research Systems MacLeod-Boynton color space was used. This color space uses the Smith and Pokorny (1975) cone fundamentals and transform matrices from Travis (1991). Subjects responded using a CB6 Push Button Response Box (Cambridge Research Systems).

Between Experiments 1 and 2 new lab equipment was purchased, and the old equipment was retired. Thus, in Experiment 2, stimuli were again programmed in MATLAB but were presented on a Cambridge Research Systems Display++ 32-inch LED-backlit LCD monitor in ViSaGe mode (100-Hz refresh rate, 1440 × 1080 usable pixel resolution corresponding to 524 × 393 mm). The Display++ continuously measures and maintains its luminance output. The monitor was allowed to warm up for at least 30 minutes with full screen white at 60 cd/m^2.

For all phases of both experiments, subjects viewed the stimuli binocularly. Testing took place in a dark windowless room, with subjects' heads placed in a chin rest situated 57 cm from the monitor. Subjects were

dark adapted for only the few minutes required to set up a block of trials; however, the room lights were kept off for the duration of the experiment.

Public registration

Experiment 1 was registered with the Open Science Framework (https://cos.io/prereg/) before data collection had been completed but after four subjects were tested for pilot data for a grant proposal to the National Science Foundation. In the pre-registration, the author proposed analyzing the data via two-way analyses of variance (ANOVAs) in each color plane (stimulus type × cardinal/non). The author hypothesized an interaction where gratings should yield evidence for separate mechanisms (aligned/orthogonal threshold ratios >1) for the cardinal and non-cardinal colors, but spots should only do so for cardinal colors; however, on further thought, a more direct test was chosen: one-sample *t*-tests of threshold ratios against 1. In addition, the threshold ratios for spots versus gratings were compared for the non-cardinal colors in paired *t*-tests to determine if the gratings do yield higher threshold ratios, as hypothesized. These are the analyses that are presented in this paper. De-identified data for Experiment 1 and graphs of individual subjects' data for Experiment 2 are available at https://osf.io/ag8vr/. Experiment 2 was not pre-registered.

Individualization of stimulus parameters

Three aspects of the stimuli were individualized for each subject: (1) the luminance ratio of the two phases of the isoluminant S-axis stimuli, (2) the threshold contrasts of each mask, and (3) the orientation of the non-cardinal stimuli in equal threshold space.

Aspects of the visual system are known to vary across people with normal color vision, which can introduce variability in how sensitive people are to different colors. For example, macular pigment, located around the fovea of the retina, preferentially absorbs wavelengths below 520 nm and varies across subjects (Bone, Landrum, & Cains, 1992; Wooten & Hammond, 2005); thus, it can differentially impact the relative luminance values of the S+ and S– phases of the gratings. Due to these individual differences, use of the same stimuli across all subjects would introduce luminance artifacts in the stimuli, making the cardinal S stimuli actually slightly non-cardinal (i.e., not bluish/yellowish but rather intense-bluish/dim-yellowish or intense-yellowish/dim-bluish). Thus, to avoid luminance artifacts, the S+ and S– phases were set to be isoluminant via heterochromatic flicker photometry (Ives, 1912) for each subject individually (see Determining isoluminance sections, below).

A second aspect of the visual system that can vary in sensitivity across subjects is the neural pathways that underlie the detection of S and L+M. Activities such as playing action video games can improve contrast sensitivity and thus introduce variability in sensitivity across subjects (Li, Polat, Makous, & Bavelier, 2009). To ensure that these two stimuli were equally salient, thresholds to detect both cardinal color axes (S and L+M) were determined for each subject. Noise masks were then presented at multiples of each subject's threshold to detect each color (see Determining contrast thresholds sections, below).

The non-cardinal colors were also individualized for each subject, by creating them in equal threshold space, as we (Gunther, 2014a; Gunther, 2014b; Gunther & Dobkins, 2003; Gunther & Downey, 2016) and others (Krauskopf & Gegenfurtner, 1992; Krauskopf, Wu, & Farell, 1996; Li & Lennie, 1997; Webster & Mollon, 1994) have done before (see Individualizing non-cardinal colors section, below).

Experiment 1

Determining isoluminance

Stimuli

The stimuli used to determine isoluminance were vertically oriented sine-wave Gaussian-filtered gratings ($SD = 1$), with 8° visual angle diameter. The spatial frequency was 0.5 cycles/degree (c/deg) and temporal frequency was 5 Hz (counterphase flicker). The spatial frequency was halfway between the 0 c/deg of the spot stimuli and the 1 c/deg of the gratings; Dobkins, Gunther, and Peterzell (2000) found that spatial frequency does not alter isoluminance settings within this range. For the isoluminance settings, the contrast of the S+/S– gratings was set to 40% maximum on the monitor, the contrast used in Gunther and Downey (2016). The background was a gray of the mean chromaticity and luminance for all stimuli. The same background was used in all paradigms (determining isoluminance, contrast threshold, noise masking). A black fixation dot (0.2° diameter) remained visible for the duration of the experiment. The fixation dot and the grating were centered on the monitor. The stimuli were created in MacLeod-Boynton color space (MacLeod & Boynton, 1979). The color coordinates for the cardinal colors are shown in Table 1. Rods are unlikely to have contributed to the perception of the stimuli used in this experiment, as the stimuli were presented foveally where there are fewer rods, and stimuli of the same luminance were shown to not contribute substantially to the results of Dalhaus and Gunther (2012), even in the periphery where rods are more plentiful.

Procedure

Heterochromatic flicker photometry (HFP) (Ives, 1912) was used to set the stimuli to be isoluminant. Subjects adjusted the luminance of the two phases of the stimulus (e.g., S+ and S–) until the flicker appeared minimal (the stimuli could have appeared to disappear, leaving only the mean gray background visible; the flicker could have appeared to slow; or the stimuli could have appeared to shrink). Minimal flicker occurs when the two phases are equal in luminance. Buttons on the CB6 Push Button Response Box allowed for coarse (0.5% Michelson contrast) or fine (0.1% Michelson contrast) adjustments. As the subject increased the luminance of one phase, the other decreased by the same amount, keeping the mean luminance equal to the background, at 24 cd/m^2. A separate CB6 button was used to enter the response. Subjects completed 20 trials for each color axis. Outliers (defined as Michelson settings more than 2.5 of the subject's standard deviation away from the subject's mean) were removed. If the standard deviation of the Michelson contrast of the settings was still greater than 5%, more trials were run until the most recent 20 trials met the criterion. The average isoluminance value was calculated on only the most recent 20 trials. All remaining portions of the experiment were conducted with stimuli presented at each subject's individually determined isoluminant point.

Determining contrast thresholds

Stimuli

Contrast thresholds were determined using both 8°-diameter 1 c/deg sine-wave Gaussian-filtered gratings and an 8°-Gaussian spot. The gratings were presented for 2 seconds, ramping on and off in contrast to avoid sharp temporal edges. The stimuli appeared 2° either left or right of a centrally located fixation dot (black, 0.2° diameter). In the noise masking paradigm below, the stimulus and the noise mask were presented on alternate refreshes of the monitor. This halved the contrast of the stimuli. Therefore, the contrast thresholds were determined in the presence of a "mask" of the background gray color; this mask was not readily apparent, but it did reduce the contrast the same amount as the real noise masks did, so the contrasts determined here transferred to the noise masking paradigm below. Contrast thresholds were determined for the two cardinal axes: S and L+M (see Table 1 for color coordinates).

Color	S	M–L	Luminance (cd/m^2)
S+ (bluish)	0.028	0.335	24
S– (yellowish)	0.004	0.335	24
–(L+M) (black)	0.016	0.335	2
L+M (white)	0.016	0.335	46
Gray background	0.016	0.335	24

Table 1. MacLeod–Boynton color space coordinates of cardinal stimuli, Experiment 1.

Procedure

Three hundred trials were presented for each color axis tested: 30 trials at each of 10 contrasts. Contrasts were chosen to bracket the average threshold; Blake and Sekuler (2006) recommended at least 20 trials per contrast. Subjects initiated each trial. One stimulus, at one contrast, appeared for 2 seconds at one location (left or right of fixation), randomly chosen. The subject then reported whether the stimulus was on the left or right. Subjects were allowed a few practice trials until they felt comfortable with the task, then the 300 trials were started. Feedback was not given. After the block of trials was complete, the 75% contrast threshold was determined using a 10-point sigmoidal best-fitting function. Each color axis was presented in a separate block of trials.

Individualizing non-cardinal colors

When the contrast thresholds for the cardinal stimuli (S and L+M) had been determined, the non-cardinal colors were set to be halfway (45° and 135° in color space) between the cardinal axes in equal threshold space; see Appendix A for details. This ensures that if the non-cardinal colors are detected not by specific non-cardinal mechanisms but instead by the cardinal mechanisms then the stimuli would equally stimulate the two neighboring cardinal mechanisms.

Noise masking

Stimuli

The target stimuli were either 8°-diameter Gaussian spots, or 8°-diameter Gabor gratings of 1 c/deg spatial frequency. The value of 1 c/deg for the grating stimulus was chosen to be intermediate between the 0.5 c/deg of Stoughton et al. (2012) and the 1.2 c/deg of Gegenfurtner and Kiper (1992). The stimuli flickered at 5 Hz between the two endpoints of the color axis being tested (e.g., S+ and S–). The stimuli appeared centered 2° either left or right of the centrally located fixation dot (black, 0.2° diameter), as they were for determining contrast thresholds.

The noise mask consisted of a 20° × 10° horizontal rectangle (centered on fixation), filled with 0.2° ×

0.2° square dots of white noise varying between the two endpoints of the color axis being tested. The counterphase of the dots flickered at a rate of 5 Hz. The locations of the noise dot contrasts were re-randomized on each trial. The mask contrast was set to 5 times the subject's threshold to detect that color axis (see Determining contrast thresholds sections, above). The noise mask remained visible for the duration of the block of 300 trials.

The target stimulus and the noise mask were interleaved on alternating refreshes of the monitor. At a refresh rate of 100 Hz, the target and noise stimuli appeared to coexist.

Procedure

Thresholds to detect stimuli, when embedded in aligned or orthogonal noise, were determined as described above for the procedure for determining contrast thresholds. Sixteen noise-masked thresholds were determined. The four color axes (S and L+M cardinal and 45° and 135° non-cardinal) were presented in aligned noise (e.g., S stimulus in S noise) or in orthogonal noise (e.g., S stimulus in L+M noise). Note that cardinal stimuli were only presented in cardinal noise, and non-cardinal stimuli were only presented in non-cardinal noise. These eight stimuli (four color axes, presented in both aligned and orthogonal noise) were presented both as spots and as gratings. These 16 stimulus conditions were presented in random order in separate blocks.

Experiment 2

Experiment 2 tested the same two cardinal and two 45° non-cardinal masks per color plane as in Experiment 1. Here, multiple stimulus directions were tested in each mask. Subject KLG was tested in 12 stimulus directions spaced at 15° increments in each color plane. Subjects IT and NHJ were tested in eight stimulus directions spaced at 22.5° increments. The change in equipment between Experiments 1 and 2 necessitated a change in color space and thus how the stimuli were set up. The specifics of creating the stimuli for Experiment 2 are explained in Appendix B.

Results

Experiment 1

Evidence of independent, orthogonal mechanisms is indicated by a larger masking effect with aligned noise (e.g., S stimulus in S noise) than the masking

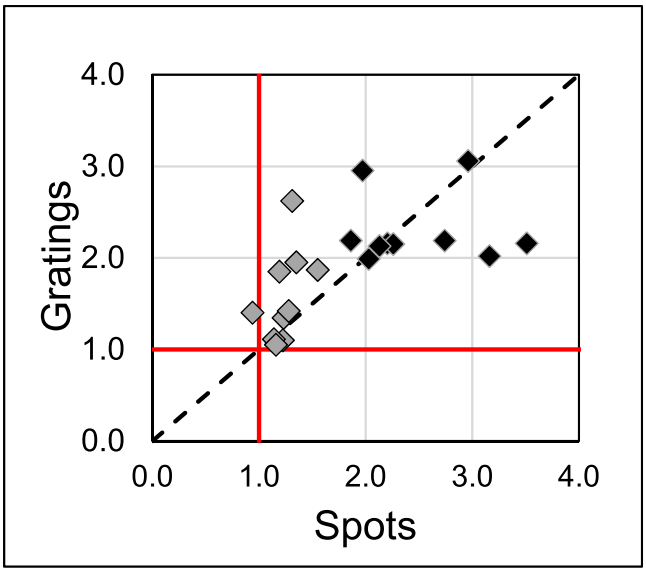

Figure 2. Results from Experiment 1. Data for cardinal stimuli are shown in black (averaged across the two cardinal stimuli), and those for non-cardinal stimuli are shown in gray (averaged across the two non-cardinal stimuli). Aligned/orthogonal ratios for spots are plotted along the *x*-axis and for gratings along the *y*-axis. Spot data to the right of the solid red line or grating data above the solid red line indicate evidence for separate underlying mechanisms (aligned/orthogonal ratio > 1.0). Symbols above the black dashed line indicate stronger evidence for non-cardinal mechanisms when using gratings than when using spots.

caused by the orthogonal noise (e.g., S stimulus in L+M noise). This would be shown by the symbols in Figure 2 being greater than 1.0. This is hypothesized to be the case for the cardinal stimuli (black symbols to the right and above the solid red lines) for both the spots and the gratings, and for the non-cardinal stimuli with the gratings (gray symbols above the solid red horizontal line). The non-cardinal spots (gray symbols plotted along the *x*-axis) should in particular stimulate LGN mechanisms (Conway et al., 2010), where primarily only cardinal mechanisms are known to exist (Gegenfurtner, 2003) (but c.f. Tailby et al., 2008; Wool et al., 2019). Thus, both aligned and orthogonal noise should tap both cardinal mechanisms, causing the same amount of interference. This means that thresholds for non-cardinal spots in aligned and orthogonal noise are expected to be similar, yielding a ratio of close to 1.0 in Figure 2 (gray symbols clustering around the solid red vertical line).

In the S versus L+M color plane (the color plane where, to the best of the author's knowledge, this question has not yet been addressed), the results are mostly consistent with the hypothesis. The non-cardinal spot stimulus mean (1.24 ± 0.16; gray symbols plotted along the *x*-axis) is significantly greater than 1.0

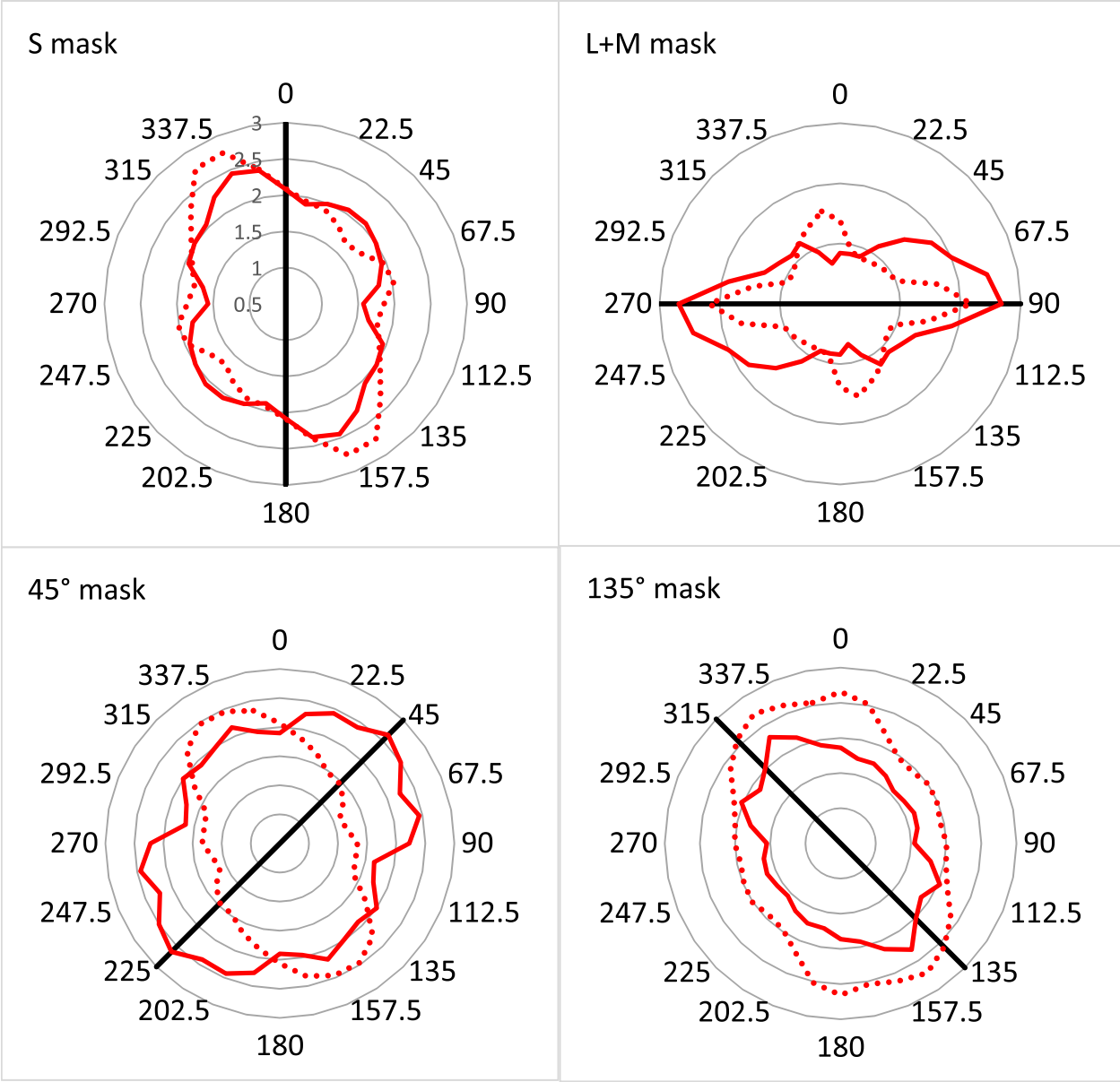

Figure 3. Data for Experiment 2. Each graph represents a different mask. Radial lines represent 0.5× baseline threshold. Dotted red lines represent spot stimuli, and solid red lines represent grating stimuli, all plotted as weighted group averages (see text). Straight black lines represent the direction of the mask.

[$t(9) = 4.773$; $p = 0.001$; Cohen's $d = 1.51$; 95% confidence interval (CI) on the difference from 1.0, 0.13–0.35], largely because of the small variability. The non-cardinal grating stimulus mean (1.57 ± 0.50; gray symbols plotted along the y-axis) is also significantly greater than 1.0 [$t(9) = 3.644$; $p = 0.005$; Cohen's $d = 1.15$; 95% CI on the difference from 1.0, 0.22–0.93]. A paired t-test on the non-cardinal spot versus grating data shows that the mean for the grating stimuli is not significantly greater than the mean for the spot stimuli [$t(9) = 2.379$; $p = .041$; Cohen's $d = 0.75$; 95% CI on the difference between the means, 0.016–0.65], when factoring in a Bonferroni correction for three t-tests (Bonferroni corrected $\alpha = 0.0167$). As can be seen in Figure 2, a number of the gray non-cardinal symbols do cluster around the spot-equals-grating black dashed line, with a few above the line. In this color plane, there is thus a trend toward gratings showing stronger evidence for non-cardinal mechanisms than the spots do. Note that t-tests were conducted rather than two-way ANOVAs because the t-tests can pinpoint the comparisons of interest to the research questions.

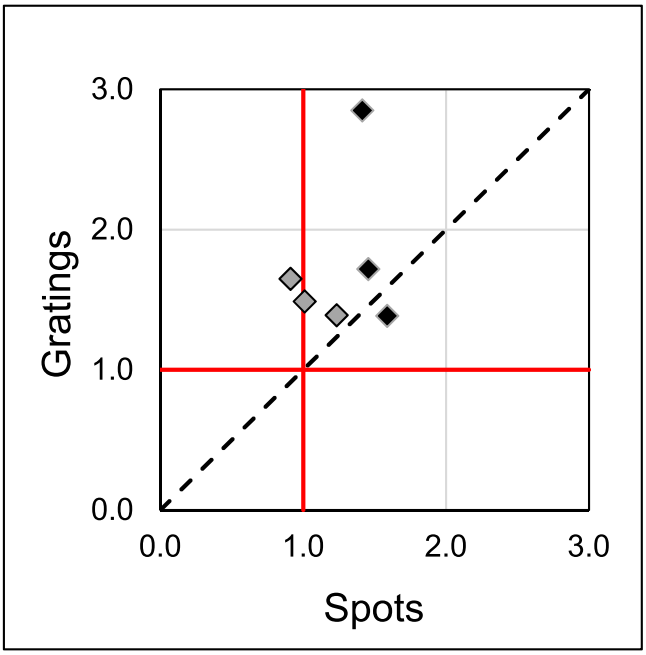

Figure 4. Results for Experiment 2, as plotted for Experiment 1 in Figure 2.

Given that there is ample evidence that there are separate mechanisms underlying the three cardinal axes (e.g., Derrington et al., 1984; Krauskopf, Williams, & Heeley, 1982), it was expected that the cardinal stimuli would yield threshold ratios > 1 for both spots and gratings. This is in fact the case, with the cardinal threshold ratios (black symbols in Figure 2) yielding $t(9) = 8.245$, $p < 0.001$ for spots and $t(9) = 10.815$, $p < 0.001$ for gratings. In addition, the paired t-tests [$t(9) = 0.842$, $p = 0.422$] do not show a preference for gratings; this is also shown in Figure 2, where the black symbols are more evenly spread on either side of the spot-equals-grating black dashed line. Statistics were not performed for Experiment 2 given the small sample size, but the black symbols in Figure 4 are also above and to the right of the solid red lines, indicating aligned/orthogonal ratios greater than 1.0, but on both sides of the spot-equals-grating black dashed line, indicating separable mechanisms with either stimulus type.

Experiment 2

The data for Experiment 2 are shown in Figures 3 and 4. In Figure 3, different masks are shown in each separate graph. Data are plotted as the ratio of the threshold to detect that particular stimulus on that particular mask (e.g., S grating on S mask) divided by the threshold to detect that same stimulus (e.g., S grating) on the gray mask. The red lines represent a smoothed, weighted average: the average threshold ratio (across all three subjects) to detect that stimulus (e.g., S grating in S mask), weighted as 1.0, averaged with half-weighting of the average threshold ratios for the neighboring two stimuli (e.g., 165° and 15° gratings, also in the S mask). Graphs of individual subject data can be found at https://osf.io/ag8vr/.

Although the data are noisy with only three subjects, a pattern similar to that seen in Experiment 1 can be seen here. Cardinal masking (top two rows in Figure 3) is stronger for aligned than orthogonal masking (vertical elongation of data in S mask graph, horizontal elongation in L+M mask graph). For the 135° non-cardinal S versus L+M mask, the oblong of data for the grating stimuli (solid red line) is oriented in the 135°/315° direction and is thinner than is the oblong of data for the spot stimuli (dotted red line). For the 45° non-cardinal S versus L+M mask, the grating data look good, but the spot data are oriented in the opposite direction (oriented in the 135° direction rather than the 45° direction).

In Figure 4, for cross-experiment comparisons, the data for Experiment 2 are plotted as they were for Experiment 1 in Figure 2. This graph plots just the cardinal and the two 45° non-cardinal color directions. The data nicely fit the hypothesis, with an aligned/orthogonal ratio essentially at 1.0 (1.05 ± 0.26) for the non-cardinal spots (gray symbols plotted along the x-axis), and >1.0 (1.51 ± 0.76) for the gratings (gray symbols plotted along the y-axis). All of the non-cardinal gray symbols are above the spot-equals-grating black dashed line, indicating that the aligned/orthogonal ratios are higher for gratings than for spots, in accordance with the hypothesis.

Discussion

To a large extent, the data support the hypothesis that gratings should better reveal non-cardinal mechanisms than spots do. To the best of the author's knowledge, this is the first time this question has been addressed in the S versus L+M color plane. The threshold ratio for the non-cardinal gratings was significantly greater than 1.0 in Experiment 1 (with very similar results in Experiment 2; 1.57 in Experiment 1 and 1.51 in Experiment 2). Although the mean aligned/orthogonal threshold ratio was only slightly greater than 1.0 for the non-cardinal spots in Experiment 1, it was significantly so, because of the extremely small variability across subjects. The non-cardinal spot mean was lower in Experiment 2 (1.24 in Experiment 1 versus 1.05 in Experiment 2). Although the aligned/orthogonal ratio was higher for gratings than spots in Experiment 1, it was not significantly so when a Bonferroni correction for multiple tests was factored in.

The significant aligned/orthogonal ratios for non-cardinals with spot stimuli in Experiment 1 might be due to the low variability, thus increasing the *t*-value. Alternatively, this could be a reflection of the findings of Tailby and colleagues (2008) that LGN S– neurons respond to a wide range of hues. A wide range would mean that these LGN neurons, which have circular receptive fields, are responding to non-cardinal colors.

The results for Experiment 2 are a bit weaker than those for Experiment 1. This may be due to the weaker masks in Experiment 2. Two subjects had masks at 4.5× threshold, but one subject was only able to get his S threshold low enough for a 3× mask, compared with 5× masks for Experiment 1. There is a long history of masking experiments that varied the contrast of the masks (e.g., Legge & Foley, 1980). At low mask contrasts there can even be an enhancement of performance, where thresholds are lower (sensitivity is higher) with low contrast masks, leading to what is known as a "dipper function" as mask contrast increases. Our masks, however, were not this low; none of the masked thresholds on aligned masks was lower than thresholds with the gray "mask".

Wang, Richters, and Eskew (2014) and Vingrys and Mahon (1998) have shown that S-cone increments (S+) are masked to a greater extent (by noise masks of varying color) than are S-cone decrements (S–). In addition, Gabree, Shepard, and Eskew (2018) showed that S-cone stimuli, either S+ or S–, are masked to a greater extent by S+ than S– pedestals. This might translate to greater masking of 45° non-cardinal (intense-bluish/dim-yellowish) than 135° non-cardinal (intense-yellowish/dim-bluish) stimuli. Vingrys and Mahon (1998) also found stronger masking with luminance increments than decrements; they especially found that blue plus luminance increments showed large effects of aligned masking. Figure 5 shows the data from Figure 2 separately for each color axis tested. The results obtained in Experiment 1 of the current study thus align with these other studies, as 45° non-cardinal stimuli were more strongly masked by 45° masks than by 135° masks, as shown by an average aligned/orthogonal ratio greater than 1 in Figure 5 (intense-bluish/dim-yellowish diamonds above and to the right of the solid red lines). The 135° stimuli also show this pattern; aligned/orthogonal ratios < 1 indicate stronger masking by 45° than 135°, although a smaller difference than for 45° stimuli, as shown by more of the intense-yellowish/dim-bluish diamonds being below and to the left of the solid red lines. In Experiment 2 (Figure 3), the 45° mask did provide stronger masking than did the 135° mask, as seen in the graph where the mask versus unmasked thresholds are at higher multiples (axis bands being more tightly packed) on the 45° mask than the 135° mask; this is consistent with the results from the literature. However, in Experiment 2 there was stronger aligned than orthogonal masking for both 45° and 135° gratings, rather than 45° masks always yielding stronger masking. In addition, the spot stimuli on the 45° mask actually show the opposite tuning to that found by previous studies, as the 135° spots showed stronger masking than did the 45° spots.

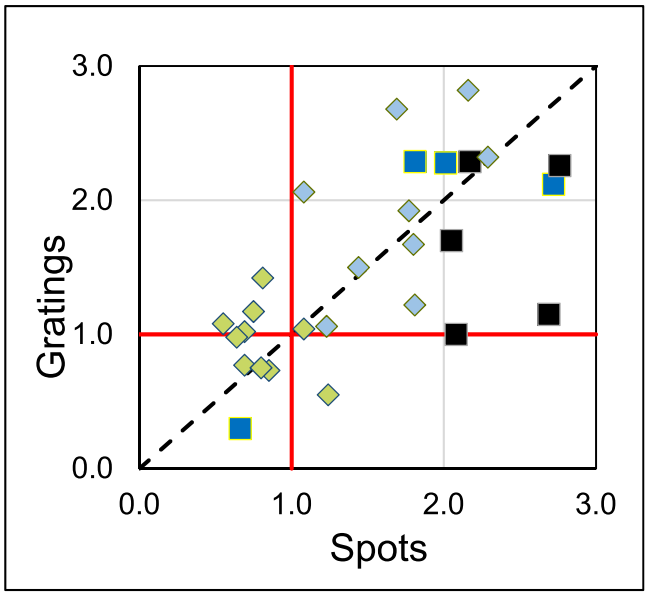

Figure 5. Results from Experiment 1 with each axis shown separately: S in blue/yellow squares, L+M in black/gray squares, 45° in intense-bluish/dim-yellowish diamonds, and 135° in intense-yellowish/dim-bluish diamonds. Other features are as described for Figure 2.

A question could be raised that perception of both spot and grating stimuli begins in the eyes, and conscious perception occurs in the cortex; thus, processing of both stimulus types passes through both the LGN and cortex. Therefore, what does it mean that spots better stimulate the LGN and gratings better stimulate the cortex? Stoughton and colleagues (2012) and Gegenfurtner and Kiper (1992) both proposed that spots versus gratings were "more effective" at stimulating LGN versus cortical neurons. If "more effective" means that these neurons reduce noise better, and thus have a stronger signal-to-noise ratio, then a higher-up decision neuron could then listen to the signal strength coming from below (LGN and cortex) and base its decision on the strongest signal. This is analogous to maximum-likelihood decoder models (e.g., Goris, Putzeys, Wagemans, & Wichmann, 2013), with the decision neuron choosing the "loudest" response, but here choosing between LGN and cortical signals rather than between neurons responding to stimulus A versus stimulus B.

One further possible concern is that the noise dots (0.2° × 0.2° in Experiment 1 and 0.4° × 0.4° in Experiment 2) are closer to the 1 c/deg spatial frequency

of the gratings (slightly more than one octave apart in Experiment 1; close to the same width [0.4° versus 0.5° for one phase of the grating] in Experiment 2) than they are to the spatial frequency of the spots (8° diameter; slightly above five octaves apart for Experiment 1 and slightly below five octaves for Experiment 2). This thus creates somewhat of a spatial frequency mask—in addition to a color mask—for the gratings but not the full-field spot stimuli. In Experiment 1, the subjects did in fact have the most trouble obtaining thresholds for gratings when presented in aligned noise (in Experiment 2 the baseline thresholds were taken on noise stimuli, not spots and gratings). However, Legge and Foley (1980) found that masks that were an octave lower than target stimuli in spatial frequency were six times less potent maskers as when the mask and target stimuli matched in spatial frequency. Further, this potential spatial frequency mask is not expected to produce an artifact that would skew the data, because the comparisons in the current study are between the cardinal and non-cardinal masking effects within each stimulus type (spot versus grating), rather than across stimulus types.

In conclusion, as had been found in the isoluminant color plane (Stoughton et al., 2012) and the L–M versus L+M color plane (Gegenfurtner & Kiper, 1992), gratings do reveal non-cardinal mechanisms better than do spots in the S versus L+M color plane, as well.

Keywords: non-cardinal color, cortex, lateral geniculate nucleus, psychophysics

Acknowledgments

Supported by a National Science Foundation grant (BCS-1753808). Any opinions, findings, and conclusions or recommendations expressed in this material are those of the author and do not necessarily reflect the views of the National Science Foundation. Help in data collection was provided by summer research interns Carson Powell (funded by the Eldon Parks Memorial Fund for support of student research in psychology) and Colby Dunigan, Jorge Rodriguez, Alex Naylor, and Isaac Temores (all funded by this National Science Foundation grant). Subject payments were provided by the National Science Foundation grant and the Daniel F. Evans Associate Professor in Social Science endowed fund. Open-access publication costs were also funded by this National Science Foundation grant.

Commercial relationships: none.
Corresponding author: Karen L. Gunther.
Email: guntherk@wabash.edu.
Address: Psychology Department, Wabash College, Crawfordsville, IN, USA.

References

Blake, R., & Sekuler, R. (2006). *Perception* (5th ed.). Boston: McGraw Hill.

Bone, R. A., Landrum, J. T., & Cains, A. (1992). Optical density spectra of the macular pigment *in vivo* and *in vitro*. *Vision Research, 32*(1), 105–110.

Boynton, R. M., & Kaiser, P. K. (1968). Vision: The additivity law made to work for heterochromatic photometry with bipartite fields. *Science, 161*(3839), 366–368.

Buck, S. L., Frome, F., & Boynton, R. M. (1977). Initial distinctness and subsequent fading of minimally distinct borders. *Journal of the Optical Society of America, 67*(8), 1126–1128.

Conway, B. R., Chatterjee, S., Field, G. D., Horwitz, G. D., Johnson, E. N., Koida, K., & Mancuso, K. (2010). Advances in color science: From retina to behavior. *Journal of Neuroscience, 30*(45), 14955–14963, https://doi.org/10.1523/JNEUROSCI.4348-10.2010.

Dalhaus, R. N., III, & Gunther, K. L. (2012). A tritan *Waldo* would be easier to detect in the periphery than a red/green one: Evidence from visual search. *Journal of the Optical Society of America A, 29*(2), A298–A305.

Derrington, A. M., Krauskopf, J., & Lennie, P. (1984). Chromatic mechanisms in lateral geniculate nucleus of macaque. *Journal of Physiology, 357*, 241–265.

DeValois, R. L., Cottaris, N. P., Elfar, S. D., Mahon, L. E., & Wilson, J. A. (2000). Some transformations of color information from lateral geniculate nucleus to striate cortex. *Proceedings of the National Academy of Sciences, USA, 97*(9), 4997–5002, https://doi.org/10.1073/pnas.97.9.4997.

Dobkins, K. R., Gunther, K. L., & Peterzell, D. H. (2000). What covariance mechanisms underlie green/red equiluminance, luminance contrast sensitivity and chromatic (green/red) contrast sensitivity? *Vision Research, 40*(6), 613–628.

Eskew, R. T., Jr. (2009). Higher order color mechanisms: A critical review. *Vision Research, 49*(22), 2686–2704.

Eskew, R. T., Jr., Newton, J. R., & Giulianini, F. (2001). Chromatic detection and discrimination analyzed by a Bayesian classifier. *Vision Research, 41*(7), 893–909.

Gabree, S. H., Shepard, T. G., & Eskew, R. T., Jr. (2018). Asymmetric high-contrast masking in S cone increment and decrement pathways. *Vision Research, 151*, 61–68, https://doi.org/10.1016/j.visres.2017.06.017.

Gegenfurtner, K. R. (2003). Cortical mechanisms of colour vision. *Nature Reviews Neuroscience, 4*(7), 563–572, https://doi.org/10.1038/nrn1138.

Gegenfurtner, K. R., & Kiper, D. C. (1992). Contrast detection in luminance and chromatic noise. *Journal of the Optical Society of America A, 9*(11), 1880–1888.

Giulianini, F., Eskew, R. T., &, Jr. (1998). Chromatic masking in the (delta L/L, delta M/M) plane of cone-contrast space reveals only two detection mechanisms. *Vision Research, 38*(24), 3913–3926, https://doi.org/10.1016/s0042-6989(98)00068-6.

Goris, R. L. T., Putzeys, T., Wagemans, J., & Wichmann, F. A. (2013). A neural population model for visual pattern detection. *Psychological Review, 120*(3), 472–496, https://doi.org/10.1037/a0033136.

Gunther, K. L. (2014a). Non-cardinal color mechanism strength differs across color planes but not across subjects. *Journal of the Optical Society of America A, 31*(4), A293–A302.

Gunther, K. L. (2014b). Non-cardinal color perception across the retina: Easy for orange, hard for burgundy and sky blue. *Journal of the Optical Society of America A, 31*(4), A274–A282.

Gunther, K. L., & Dobkins, K. R. (2003). Independence of mechanisms tuned along cardinal and non-cardinal axes of color space: Evidence from factor analysis. *Vision Research, 43*(6), 683–696.

Gunther, K. L., & Downey, C. O. (2016). Influence of stimulus size on revealing non-cardinal color mechanisms. *Vision Research, 127*, 57–66.

Hansen, T., & Gegenfurtner, K. R. (2006). Higher level chromatic mechanisms for image segmentation. *Journal of Vision, 6*(3), 239–259, https://doi.org/10.1167/6.3.5.

Hansen, T., & Gegenfurtner, K. R. (2013). Higher order color mechanisms: Evidence from noise-masking experiments in cone contrast space. *Journal of Vision, 13*(1):26, 1–21, https://doi.org/10.1167/13.1.26.

Ives, H. E. (1912). Studies in the photometry of lights of different colours - IV. The addition of luminosities of different colour. *Philosophical Magazine, 24*(144), 845–853.

Krauskopf, J., & Gegenfurtner, K. (1992). Color discrimination and adaptation. *Vision Research, 32*(11), 2165–2175.

Krauskopf, J., Williams, D. R., & Heeley, D. W. (1982). Cardinal directions of color space. *Vision Research, 22*(9), 1123–1131.

Krauskopf, J., Wu, H. J., & Farell, B. (1996). Coherence, cardinal directions and higher-order mechanisms. *Vision Research, 36*(9), 1235–1245.

Legge, G. E., & Foley, J. M. (1980). Contrast masking in human vision. *Journal of the Optical Society of America, 70*(12), 1458–1471.

Li, A., & Lennie, P. (1997). Mechanisms underlying segmentation of colored textures. *Vision Research, 37*(1), 83–97.

Li, R., Polat, U., Makous, W., & Bavelier, D. (2009). Enhancing the contrast sensitivity function through action video game training. *Nature Neuroscience, 12*(5), 549–551. https://doi.org/10.1038/nn.2296.

MacLeod, D. I. A., & Boynton, R. M. (1979). Chromaticity diagram showing cone excitation by stimuli of equal luminance. *Journal of the Optical Society of America, 69*(8), 1183–1186.

Parry, N. R. A., & Robson, A. G. (2012). Optimization of large field tritan stimuli using concentric isoluminant annuli. *Journal of Vision, 12*(12):11 1–13 https://doi.org/10.1167/12.12.11.

Sankeralli, M. J., & Mullen, K. T. (1997). Postreceptoral chromatic detection mechanisms revealed by noise masking in three-dimensional cone contrast space. *Journal of the Optical Society of America A, 14*(10), 2633–2646.

Smith, V. C., & Pokorny, J. (1975). Spectral sensitivity of the foveal cone photopigments between 400 and 500 nm. *Vision Research, 15*(2), 161–171.

Smith, V. C., & Pokorny, J. (1995). Chromatic-discrimination axes, CRT phosphor spectra, and individual variation in color vision. *Journal of the Optical Society of America A, 12*(1), 27–35.

Smith, V. C., Pokorny, J., & Pass, A. S. (1985). Color-axis determination on the Farnsworth-Munsell 100-hue test. *American Journal of Ophthalmology, 100*(1), 176–182.

Smithson, H. E. (2014). S-cone psychophysics. *Visual Neuroscience, 31*(2), 211–225, https://doi.org/10.1017/S0952523814000030.

Stockman, A. (2019). Cone fundamentals and CIE standards. *Current Opinion in Behavioral Sciences, 30*, 87–93.

Stockman, A., & Sharpe, L. T. (2000). The spectral sensitivities of the middle- and long-wavelength-sensitive cones derived from measurements in observers of known genotype. *Vision Research, 40*(13), 1711–1737.

Stoughton, C. M., Lafer-Sousa, R., Gagin, G., & Conway, B. R. (2012). Psychophysical chromatic mechanisms in macaque monkey. *Journal of Neuroscience, 32*(43), 15216–15226, https://doi.org/10.1523/JNEUROSCI.2048-12.2012.

Tailby, C., Solomon, S. G., & Lennie, P. (2008). Functional asymmetries in visual pathways carrying S-cone signals in macaque. *Journal*

of Neuroscience, 28(15), 4078–4087, https://doi.org/10.1523/JNEUROSCI.5338-07.2008.

Tansley, B. W., & Boynton, R. M. (1978). Chromatic border perception: The role of red- and green-sensitive cones. *Vision Research, 18*(6), 683–697.

Travis, D. (1991). *Effective colour displays: Theory and practice (computers and people)*. New York: Academic Press.

Vingrys, A. J., & Mahon, L. E. (1998). Color and luminance detection and discrimination asymmetries and interactions. *Vision Research, 38*(8), 1085–1095.

Wang, Q., Richters, D. P., & Eskew, R. T., Jr. (2014). Noise masking of S-cone increments and decrements. *Journal of Vision, 14*(13):8, 1–17, https://doi.org/10.1167/14.13.8.

Webster, M. A., Miyahara, E., Malkoc, G., & Raker, V. E. (2000). Variations in normal color vision. I. Cone-opponent axes. *Journal of the Optical Society of America A, 17*(9), 1535–1544, https://doi.org/10.1364/josaa.17.001535.

Webster, M. A., & Mollon, J. D. (1994). The influence of contrast adaptation on color appearance. *Vision Research, 34*(15), 1993–2020.

Wool, L. E., Packer, O. S., Zaidi, Q., & Dacey, D. M. (2019). Connectomic identification and three-dimensional color tuning of S-OFF midget ganglion cells in the primate retina. *Journal of Neuroscience, 39*(40), 7893–7909, https://doi.org/10.1523/JNEUROSCI.0778-19.2019.

Wooten, B. R., & Hammond, B. R., Jr. (2005). Spectral absorbance and spatial distribution of macular pigment using heterochromatic flicker photometry. *Optometry & Vision Science, 82*(5), 378–386.

Appendix A: Creation of non-cardinal colors in Macleod-Boynton color space (Experiment 1)

Equal threshold space was created by determining the number of multiples of thresholds that fit into 100% for the less-sensitive cardinal axis (e.g., subject CKD's S spot threshold was 14.89 and L+M spot threshold was 2.31, yielding a maximum multiple of 6.7). For the intense-bluish pole of the 45° S versus L+M non-cardinal stimulus, the S coordinate was set to .028 for CKD (maximum for the S coordinate). The L+M coordinate was set to 27.7 cd/m^2: 24 cd/m^2 L+M coordinate for mean white + (2.31 threshold × 6.7 multiple/100) × 24 cd/m^2 L+M extent from mean white to white pole – 0.01 cd/m^2 adjustment for his isoluminance setting. Analogous computations were performed for the other poles of the 45°/135° non-cardinal stimuli.

Appendix B: Stimulus set-up in DKL color space (Experiment 2)

Because of the change in equipment between Experiments 1 and 2, in Experiment 2 the stimuli were created in DKL color space (Derrington et al., 1984) using the Cambridge Research Systems demoGetColourTrivalRGBfromDKL function and inserting the spectra from the lab's specific Display++ that were measured with the PR-655, convolved with the Stockman and Sharpe (2000) 2° cone fundamentals. The 2° fundamentals were chosen over the 10° fundamentals because, although the stimuli are embedded in a 20° × 10° horizontal rectangular noise mask, subjects are assumed to have frequently foveated the stimuli. In determining the 10° cone fundamentals, Stockman and Sharpe's subjects were instructed to attend to 10°, not to the fovea (Stockman, 2019). The DKL color space coordinates are radius (contrast or saturation), azimuth (hue), and elevation (luminance); the color coordinates for each cardinal axis are presented in Table 2. These CIE coordinates are the mean PR-655 measurements across seven readings taken across the span of subject testing. The radii are limited by being able to test subjects at the large range of luminance values needed for the non-cardinal stimuli. The background gray was set to 0.5, 0.5, 0.5 in RGB space to maximize the size of the gamut.

Individualization of S-axis azimuth

Variations in macular pigment have been shown to affect the azimuth of the S color axis (Smith & Pokorny, 1995; Webster, Miyahara, Malkoc, & Raker, 2000), in addition to affecting isoluminance as mentioned in Experiment 1. Due to these individual differences, the azimuth of the S stimulus (the tilt within the chromatic plane of DKL space; colored in Figure 1) was set individually for each subject (an additional control over that done in Experiment 1).

Stimuli

The stimuli consisted of horizontally abutting S+ and S– 4° × 4° squares, centered vertically and horizontally on the monitor and presented on a mean gray background (see Table 2 for color coordinates; radius was set to 0.1 for determining the S-axis

	DKL Coordinates			CIE Coordinates		
Color	Radius	Azimuth	Elevation	*x*	*y*	cd/m^2
S+ (bluish)	0.3	270	0	0.2867	0.2813	60.59
S– (yellowish)	0.3	90	0	0.3595	0.4683	61.33
–L–M (black)	−0.25	180	90	0.3159	0.3553	46.12
L+M (white)	0.25	180	90	0.3147	0.3501	76.10
Gray background	0	180	90	0.3150	0.3532	61.15

Table 2. Coordinates of cardinal stimuli, Experiment 2.

azimuth). On each trial, the azimuth started at a random tilt between 265°/85° (S+/S–) and 275°/95°. On odd trials, the stimuli started with S+ on the left; even trials started with S– on the left. Borders have been shown to fade upon fixation, especially borders along the S-axis (Buck, Frome, & Boynton, 1977); thus, if the subject paused on making adjustments, the colors of the stimuli swapped sides every two seconds.

Procedure

Minimally distinct border (MDB) (Boynton & Kaiser, 1968) was used to adjust the azimuth of the S stimulus, as per Parry and Robson (2012); see also Tansley and Boynton (1978) for the application of MDB for defining the S-axis (i.e., the tritanopic confusion line). Subjects adjusted the azimuth of the stimulus by pressing buttons on the CB6 Push Button Response Box that allowed for coarse (1° azimuth) or fine (0.333° azimuth) adjustments. A separate CB6 button was used to enter the response. Subjects completed 20 trials. If the standard deviation of the settings was greater than 2° azimuth, more trials were run until the most recent 20 trials met the criterion. The average azimuth was calculated on only the most recent 20 trials. All remaining portions of the experiment were conducted with stimuli presented at each subject's individually determined S-axis azimuth.

Determining isoluminance

Stimuli

The same stimuli used in Experiment 1 were used here, with the exceptions of being created in DKL color space rather than MacLeod-Boynton color space, at an average luminance of 60 cd/m^2 rather than 24 cd/m^2, and the Gaussian-filtered sine wave gratings had a standard deviation of 2 rather than 1 to increase the apparent size of the stimuli in order to facilitate obtaining contrast thresholds. Colors were as shown in Table 2, but with the S radius at 0.1.

Procedure

As in Experiment 1, HFP was used to determine the isoluminance of the S cardinal axis. Subjects adjusted the elevation of the two phases of the stimulus (e.g., S+ and S–) until the flicker appeared minimal. Buttons on the CB6 Push Button Response Box allowed for coarse (1° elevation for S) or fine (0.2° elevation for S) adjustments. As the subject increased the luminance of one phase, the other decreased by the same amount, keeping the mean luminance equal to the background (at 0° elevation, approximately 60 cd/m^2). A separate CB6 button was used to enter the response. As in Experiment 1, subjects completed 20 trials. If the standard deviation of the settings was greater than 2° elevation for S stimuli, more trials were run until the most recent 20 trials met the criterion. The average elevation was calculated on only the most recent 20 trials. All remaining portions of the experiment were conducted with stimuli presented at each subject's individually determined elevation.

Determining cardinal contrast mask thresholds

Stimuli

These thresholds were used to both set the non-cardinal stimulus colors and to present the noise masks at 4.5× or 3× each subject's threshold. (4.5× for KLG and NHJ, 3× for IT, who had difficulty getting his thresholds low enough for a 4.5× mask.) These thresholds were determined on noise mask stimuli. The stimuli consisted of 10° × 10° squares comprised of 0.4° × 0.4° white noise squares varying between the two endpoints of the color axis being tested (e.g., varying between S+ and S–). The stimuli appeared 4° to the left or right of the central fixation dot. In the noise masking (described below), the spot or grating stimuli were presented on alternate refreshes of the monitor, thus halving the perceived contrast of the stimuli. For this reason, the cardinal noise mask thresholds were determined with the cardinal noise masks presented on alternate refreshes with a background gray mask.

Procedure

The same procedure that was used in Experiment 1 to determine contrast thresholds was used in Experiment 2.

Individualizing non-cardinal colors

Non-cardinal stimuli were created in equal threshold space for each subject individually, based on the cardinal color noise mask thresholds. Ten non-cardinal directions in each color plane, at 15° increments, were set for subject KLG; six non-cardinal directions in each color plane, at 22.5° increments, were set for the other two subjects. Cambridge Research Systems has created the DKL space such that, when the elevation is 90, the stimulus will be achromatic. The radius then defines how bright white (positive radii) or dark black (negative radii) the stimulus will be. This means that luminance for the luminance axis is adjusted by manipulating radius, but luminance for the chromatic axes is adjusted by manipulating elevation. In order to be able to create the non-cardinal axes in the S versus L+M color plane, a common metric for luminance was required. This was performed by measuring the luminance of the stimuli with a PR-655 photometer, calculating the needed luminance adjustment for each non-cardinal axis, then converting back to degrees elevation to create the stimuli in DKL space. The relationship between radius and luminance (in cd/m^2, as measured by the PR-655) for the luminance stimuli was linear (r^2 = 0.9984). However, the relationship between degree elevation and luminance for the chromatic stimuli was nonlinear. The best fit (operationalized as the highest r^2) for the relationship between degrees elevation and luminance (measured with the PR-655, averaged across four days of repeated measurements) was a third-order polynomial ($r^2 = 0.9987$).

To create the non-cardinal stimuli, first the luminance of the luminance stimuli was measured with the PR-655, from a radius of −0.25 to +0.25, on four separate days; the measurements were highly consistent across days. To figure out how much luminance to add to create each non-cardinal color, first the number of multiples of the S threshold that fit into 100% contrast were calculated (e.g., for KLG, with an S mask threshold of 20.63, this yielded a multiple of 4.85). To create equal threshold space, the luminance radius corresponding to 4.85 times the luminance mask threshold was calculated. For example, KLG's luminance threshold was 4.46% of maximum, or a radius of 0.011; when scaled up by 4.85 times, this corresponded to a radius of 0.054. The luminance (in cd/m^2) corresponding to this radius was then calculated from the linear relationship between radius and measured luminance (e.g., for KLG this yielded a luminance change of 3.35 cd/m^2). This can be thought of as the *y*-axis, with the S threshold forming the *x*-axis. The percent luminance change required for each non-cardinal direction (e.g., 15° intense S) was calculated from the sine of the angle (e.g., sin[15°]/sin[90°] = 25.88%) and added to the mean luminance for S. For example, for KLG, 0.2588 × 3.35 + 60.60 cd/m^2 mean S = 61.47 cd/m^2; note that this mean S luminance differs slightly from that in Table 2, as this reading was taken on a different day. The desired 61.47 cd/m^2 for KLG's 15° intense bluish (S+) stimulus was plugged into the third-order polynomial to determine the degrees elevation. Before determining the degrees elevation required for the non-cardinal stimuli, the required non-cardinal luminance setting was adjusted by the luminance change due to the isoluminant setting. The third-order polynomial was again used now to determine the luminance adjustment (in cd/m^2) corresponding to the psychophysically determined isoluminant elevation adjustment (e.g., KLG's S+ isoluminant adjustment of −0.13° elevation translated to −0.331 cd/m^2). This adjustment was scaled for the non-cardinal degree elevation (e.g., 15° non-cardinal = 0.2588 × [−0.331] = −0.0086 cd/m^2). Correcting the above-calculated luminance change for the 15° intense S stimulus with this isoluminance adjustment yielded the final luminance for the 15° intense S stimulus (e.g., 61.46 cd/m^2 for KLG), and thus a final 15° intense S degree elevation of 2.04°. A similar procedure was used to create the other non-cardinal stimuli in equal-threshold space.

These non-cardinal color coordinates were then used to create the 45° and 135° noise masks and the spot and grating stimuli so that all three stimulus types would have the same chromaticity at each direction in color space, enhancing the ability of the masks to mask the stimuli. Thresholds to detect the noise masks were psychophysically measured for the 45° and 135° non-cardinal directions, so that the masks could be presented at 3 times or 4.5 times (depending on the subject) each subject's threshold in the noise masking procedure below.

Noise masking

Stimuli

The target stimuli consisted of the two cardinal directions and ten non-cardinal directions spaced every 15° in the color plane (for KLG), or two cardinal plus six non-cardinal directions spaced every 22.5° (for the other two subjects). The radius for each color direction was set to slightly under the maximum possible for each color. The same 8° diameter, 1-c/deg sine wave grating, and 8° diameter spot used in Experiment 1 were used here, with the exception of the Gaussian filter standard deviation being increased to 2, as for determining isoluminance above.

The same noise mask that was used above for determining the cardinal contrast mask thresholds was used here. The noise masks were from the two cardinal and two 45°/135° non-cardinal directions that were used in Experiment 1, plus a gray baseline mask (same color

as the background). As described above, the masks were created in each subject's equal threshold color space and were presented at 3 or 4.5 times each subject's threshold to detect each non-cardinal direction.

Procedure

The same procedure as in Experiment 1 was used in Experiment 2 to determine thresholds to detect the stimuli when embedded in noise. The 120 thresholds (12 stimulus color directions times five mask directions for both spot and grating stimuli for subject KLG) for each color plane (or 80 thresholds per color plane for the other two subjects) were presented in random order within each color plane.